Mechanism of silver(I)-catalyzed Mukaiyama aldol reaction: active species in solution in AgPF$_6$-(*S*)-BINAP versus AgOAc-(*S*)-BINAP systems

Munetaka Ohkouchi, Dai Masui, Motowo Yamaguchi, Takamichi Yamagishi*

*Department of Applied Chemistry, Graduate School of Engineering, Tokyo Metropolitan University,
Minami-Ohsawa Hachioji, Tokyo 192-0397, Japan*

Abstract

Silver(I)-diphosphine complex is an effective catalyst for Mukaiyama Aldol reaction in polar solvents. AgPF$_6$-(*S*)-BINAP cationic chiral complex indicated a good activity and could afford fairly high enantioselectivity in the reaction of aromatic aldehydes and silyl enol ethers. On the other hand, AgOAc-(*S*)-BINAP system afforded the aldol product of the absolute configuration opposite to that by AgPF$_6$-(*S*)-BINAP and very high catalytic activity was shown. The structure and equilibrium state of Ag(I)-BINAP complexes in solution were examined to understand the reaction mechanism. In AgPF$_6$ system [Ag((*S*)-BINAP)$_2$]PF$_6$ (**1a**), [Ag((*S*)-BINAP)]PF$_6$ (**1b**), [Ag$_2$((*S*)-BINAP)](PF$_6$)$_2$ (**1c**) and AgPF$_6$ are present in solution. The active species of the aldol reaction in DMF is [Ag((*S*)-BINAP)]PF$_6$ (**1b**), which exists as a minor species in solution. For this cationic Ag(I) catalyst, cyclic transition state containing substrate and silyl enol ether is assumed. In AgOAc-(*S*)-BINAP system, active species is also monomeric AgOAc((*S*)-BINAP) (**2b**) species which exists as a major component in solution and strong interaction was observed with a silyl enol ether. The reaction by AgOAc-(*S*)-BINAP catalyst is concluded to proceed as follows: nucleophile forms a complex with AgOAc-(*S*)-BINAP species and is activated. This complex attacks aldehydes to afford aldol adduct via acyclic transition state. © 2001 Elsevier Science B.V. All rights reserved.

*Keywords:* Mukaiyama aldol reaction; AgPF$_6$-(*S*)-BINAP systems; AgOAc-(*S*)-BINAP systems

1. Introduction

Mukaiyama aldol reaction is one of the very useful methods for organic synthesis to construct a C–C linkage [1–3]. Many Lewis acid catalysts were developed for this reaction, such as titanium [4–9], tin [10–14], boron [15–19]. However, these catalysts require low temperature, dry conditions and relatively low substrate/catalyst ratio for obtaining aldol products in high yield and high stereoselectivities, since these Lewis acid catalysts are easily hydrolyzed by water and reaction activity is lost. Although, transition metals have weak Lewis acidity, some of them are air-insensitive, can be handled in air and are stable in the presence of water. Therefore, development of transition metal complex catalyst will be important to cultivate the new possibility of this reaction. These transition metal catalysts could work in water-containing solvent or in protic solvent where strong Lewis acids easily lose their activity. Recently,

* Corresponding author. Tel.: +81-426-77-2847;
fax: +81-426-77-2821.
E-mail address: yamagisi@ecomp.metro-u.ac.jp (T. Yamagishi).

several transition metal catalysts were reported for the Mukaiyama aldol reaction: Sodeoka et al. reported Pd-catalyzed reaction in wet DMF [20,21], and Kobayashi et al. reported Sc-catalyzed reaction in wet THF [22–27]. Although, most of previous Lewis acid catalysts require halogen-containing solvent such as $CHCl_3$ or CH_2Cl_2 for the reaction, these transition metal catalysts enabled the reaction to proceed in non-halogen solvent such as DMF and THF.
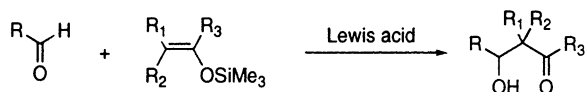
Silver(I)-catalyzed reactions were also reported. Ito et al. reported silver(I)-BPPFA catalyzed asymmetric aldol reaction of isocyanides with aldehyde [28–31]. Yanagisawa and Yamamoto et al. reported Ag(I)-BINAP catalyzed asymmetric allylation of aldehyde using allylbutyltin [32,33] and asymmetric aldol reaction between aldehyde and tin enolate [34,35]. They also reported AgF-BINAP catalyzed asymmetric aldol reaction between aldehyde and trimethoxysilyl enol ether to afford high enantioselectivity [36].

We already reported silver(I) catalyzed asymmetric Mukaiyama aldol reaction in polar solvents [37]. Cationic Ag(I)-(S)-BINAP catalyst easily caused the reaction even in water-containing DMF or THF and afforded the aldol product in a quantitative yield and in high enantioselectivity of up to 80% e.e. In this

system, the cationic character of the catalyst is important for obtaining high activity and enantioselectivity and $AgPF_6$-(S)-BINAP afforded the best results. In AgOAc-(S)-BINAP system, which is not likely to afford cationic species, much higher catalytic activity was observed and the preferential absolute configuration of the aldol product was reversed although optical yield was low.
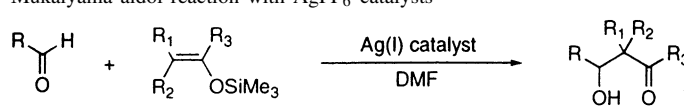
We became interested in the difference between $AgPF_6$ and AgOAc systems. We examined the structure of the active Ag(I)-BINAP species in solution and the solid state structure of Ag(I)-BINAP complexes in order to understand the reaction mechanism of the Ag(I)-catalyzed Mukaiyama aldol reaction.

2. Results and discussion

2.1. Reaction with $AgPF_6$ and AgOAc catalysts

Tables 1 and 2 summarized the results obtained for asymmetric Mukaiyama aldol reactions between aldehydes and silyl enol ethers catalyzed by $AgPF_6$-(S)-BINAP and AgOAc-(S)-BINAP. Two catalytic systems are in a striking contrast. The absolute configurations of aldol products from aromatic aldehydes in $AgPF_6$-(S)-BINAP catalyzed reaction were opposite in all cases to those obtained by AgOAc-(S)-BINAP catalyzed reaction and the

Table 1
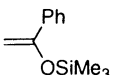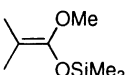Mukaiyama aldol reaction with $AgPF_6$ catalysts

Entry	Substrates	Nucleophiles	Time (h)	Yield (%)	e.e. (%)
1	PhCHO		2	100	69(S)
2[b]		Ph / OSiMe₃	96	36	80(S)
3	1-NpCHO		2	82	54(−)
4	2-NpCHO		2	100	58(−)
5	CyCHO		24	83	47(−)
6	PhCHO	OMe / OSiMe₃	24	0	

[a] Catalyst, $AgPF_6$-(S)-BINAP; solvent, DMF; temperature, 25°C; S/C/Nu = 50/1/100.
[b] The reaction performed at −30°C.

Table 2
Mukaiyama aldol reaction with AgOAc catalysts[a]

Entry	Substrates	Nucleophiles	Yield (%)			e.e. (%)
			5 min	1 h	4 h	
1	PhCHO		100			11(R)
2[b]		Ph / OSiMe₃		100 (72 h)		11(R)
3	1-NpCHO		100			17(+)
4	2-NpCHO		83	100		15(+)
5	CyCHO				100	6(+)
6	PhCHO	OMe / OSiMe₃	100			0

[a] Catalyst, AgOAc((S)-BINAP); solvent, DMF; temperature, 25°C; S/C/Nu = 50/1/100.
[b] The reaction performed at −30°C.

reaction of aliphatic aldehydes also afforded the same results. With AgPF$_6$-(S)-BINAP catalyst, the enantioselectivity was relatively high (ca. 70% e.e.) even at 25°C, while AgOAc-(S)-BINAP catalyst indicated only low enantioselectivities (ca. 10–15% e.e.). The reaction of benzaldehyde with acetophenone silyl enol ether by AgPF$_6$-(S)-BINAP proceeded fairly fast at 25°C and terminated in 2 h, but with AgOAc-BINAP the reaction proceeded extremely fast and finished in 5 min to afford 100% yield at 25°C (the substrate/catalyst ratio is 50). Using ketene silyl acetal **3** as nucleophile the AgPF$_6$ system could not cause the reaction at 25°C, but with the AgOAc system the aldol reaction also finished in 5 min to give 100% yield.

2.2. Structure of AgPF$_6$-BINAP complex in solution and solid state

We investigated the structure of AgPF$_6$-(S)-BINAP complex in solution with ^{31}P NMR method. Fig. 1a shows ^{31}P NMR spectra of AgPF$_6$-BINAP system in DMF at −50°C, where BINAP and AgPF$_6$ were mixed in 1:1 ratio. Three double doublet peaks were observed. The characterization of silver(I)-monophospine complexes in solution were performed by Muetterties and Alegranti [38], and Goel and Pilon [39]. Silver atom has two isotopes ^{107}Ag and ^{109}Ag in nature. Both of them have a nuclear spin and shows spin–spin coupling with ^{31}P atom in ^{31}P NMR spectra. They reported that spin–spin coupling
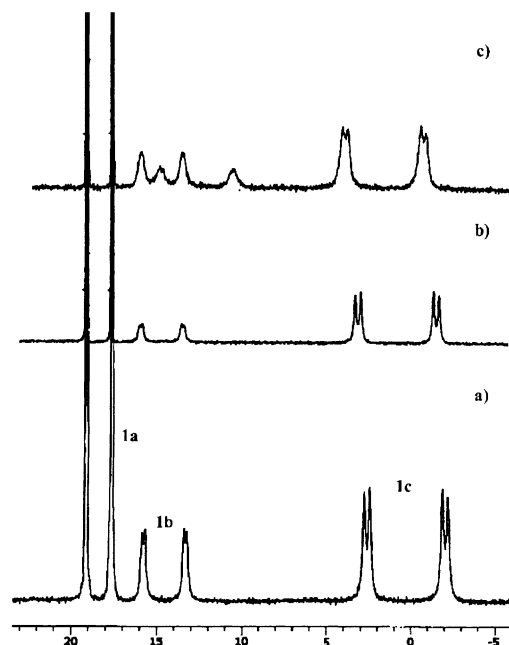

Fig. 1. ^{31}P NMR spectra of AgPF$_6$-BINAP system: (a) ^{31}P NMR spectra of AgPF$_6$-(S)-BINAP solution in DMF at −50°C; (b) benzaldehyde (50 eq.) was added to (a); (c) silyl enol ether was added to (b).

constant (J-value) between phosphorous and silver changes depending on the number of coordinated phosphorous atoms in the silver complex [38,39], and we could determine the number of coordinated

Table 3
J-values and, the number of coordinated P atoms and ligands

d (ppm)	$J_{109_{Ag}-31_P}$	$J_{107_{Ag}-31_P}$	P[a]	L[b]	Complex
−1.59	802	696	1	0.5	$[Ag_2(BINAP)](PF_6)_2$ (**1c**)
13.69	336	294	2	1	$[Ag(BINAP)]PF_6$ (**1b**)
17.46	260	224	4	2	$[Ag(BINAP)_2]PF_6$ (**1a**)

[a] The number of coordinated phosphorous atoms.

[b] The number of the coordinated ligands. Measurement at −50°C in DMF
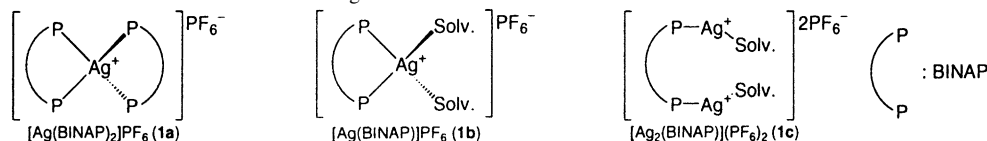
phosphorous atoms by measuring of *J*-value in ^{31}P NMR spectra.

Table 3 summarizes the obtained *J*-values of these three peaks in ^{31}P NMR spectra at −50°C and the number of coordinated phosphorous atoms on the complex species. These results show that the Ag(I) complex of 17.46 ppm has four coordinated phosphorous atoms, that is, two BINAP ligands. Therefore, this complex is $[Ag((S)$-BINAP$)_2]PF_6$ (**1a**). We prepared $[Ag((S)$-BINAP$)_2]PF_6$ (**1a**) in THF and isolated it as clear crystals (see experimental section). ^{31}P NMR of the isolated complex revealed the same peak with the in situ species of 17.46 ppm. The complex of 13.69 ppm peak and −1.59 ppm peak are considered to be $[Ag((S)$-BINAP$)]PF_6$ (**1b**) and $[Ag_2((S)$-BINAP$)](PF_6)_2$ (**1c**), respectively.
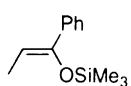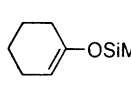
Though, $[Ag((S)$-BINAP$)_2]PF_6$ complex is a major species among Ag complexes in solution, it can not catalyze the aldol reaction and is stable in solution, not in equilibrium with other Ag(I) species. In fact, on raising the temperature to 25°C, ^{31}P NMR spectra

still revealed a sharp **1a** peak at the same position, but **1b** and **1c** peaks disappeared and new broad peak was observed at 11.7 ppm. This result shows that equilibrium exists between **1b**, **1c** and presumably AgPF$_6$.

Addition of benzaldehyde to AgPF$_6$-BINAP solution in DMF caused a change of peak style. The peak of **1b** became broad (Table 1b), while addition of silyl enol ether to AgPF$_6$-(*S*)-BINAP solution did not cause an apparent change in the spectra. Addition of silyl enol ether to the above solution containing benzaldehyde, new doublet appeared at 12.7 ppm (Fig. 1c). Thus, $[Ag((S)$-BINAP$)]PF_6$ (**1b**) is considered to interact with benzaldehyde and silyl enol ether in solution.

In the reaction of benzaldehyde with silyl enol ether **5** catalyzed by AgPF$_6$-(*S*)-BINAP, the reaction proceeded slowly in a *syn*-selective manner. *Syn*-selective reaction suggests an acyclic transition state [52–54], but slowness of the reaction for **5** suggests the cyclic transition state. For cyclic silyl enol ether **6**, the reaction did not proceed (Table 4) to afford no information

Table 4
The reaction using (*E*)- and (*Z*)-silyl enol ether[a]

Entry	Substrates	Nucleophiles	Catalyst	Time (h)	Yield	e.e. (%)	*Syn/anti*
1			AgPF$_6$-(*S*)-BINAP	24	27	–	84/16
			AgOAc-(*S*)-BINAP				
2	PhCHO			1	98	23(−)	84/16
3	PhCHO		AgPF$_6$-(*S*)-BINAP	24	0		
			AgOAc-(*S*)-BINAP				
4				3	100	1	74/26

[a] The reaction between benzaldehyde (50 eq.) and silyl enol ether (100 eq.) performed in DMF at 25°C.
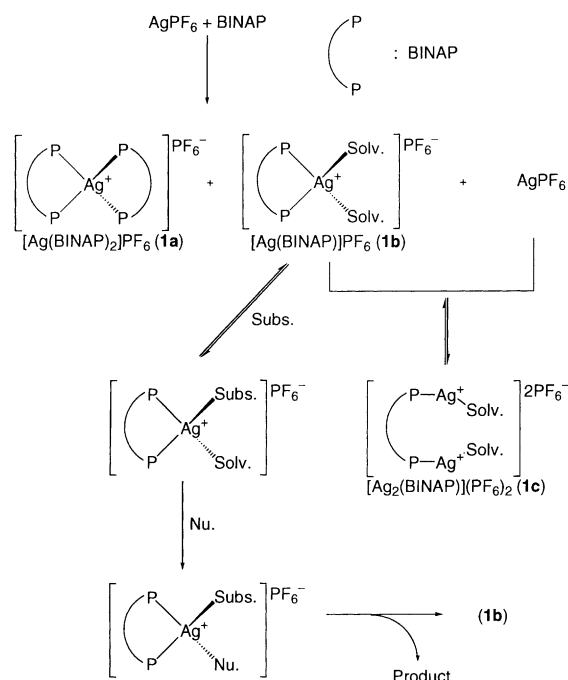
Fig. 2. Equilibrium state of AgPF$_6$-BINAP system.

2.3. Synthesis of AgOAc-diphosphine complex

We synthesized the AgOAc-diphosphine complex to understand solid state structure and equilibrium state in solution. The diphosphine ligands used were dppp, dppb, dppf, (S)-BINAP, and (S)-Tol-BINAP. We could synthesize all AgOAc-diphosphine complexes in a quantitative yield. These complexes were stable in water and can be readily handled in air.

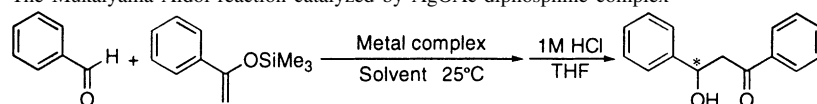### 2.4. Mukaiyama aldol reaction using AgOAc-diphosphine complex

Mukaiyama aldol reaction catalyzed by AgOAc-diphosphine complexes was examined and results were summarized in Table 5. The (S)-BINAP and (S)-Tol-BINAP complexes were effective and the reaction proceeded with 100% yield in 5 min and afforded the same results as that of in situ conditions. Triarylphosphine type ligands including dppf were more effective than alkyldiarylphosphine type ligands.

2.5. Solid state structure of AgOAc-diphosphine complex

We could obtain single crystals of AgOAc-dppb complex and AgOAc-(S)-BINAP complex by recrystallization from CH$_2$Cl$_2$–Et$_2$O and CHCl$_3$–cyclohexane, respectively. We examined the X-ray crystal structure analysis, and obtained following crystal structure and crystallographic data (Figs. 3 and 4, Table 6).

of the transition state. However, the ^{31}P NMR results indicating the interaction of Ag(I) with aldehyde and silyl enol ether and the high enantiomeric excess by AgPF$_6$-(S)-BINAP will support the cyclic transition state to afford the aldol adduct. Fig. 2 summarizes the equilibrium state in solution by AgPF$_6$-(S)-BINAP system and proposed reaction mechanism.

Table 5
The Mukaiyama Aldol reaction catalyzed by AgOAc-diphosphine complex[a]

Entry	Complex	Yield		e.e. (%)
		5 min	1 h	
1	AgOAc-(S)-BINAP	100		11(R)
2	AgOAc-(S)-Tol-BINAP	100		11(R)
3	AgOAc-dppf	100		–
4	AgOAc-dppp	88	100	–
5	AgOAc-diop	58	100	0
6	AgOAc-dppb	24	44	–
7	AgOAc-(S)-(R)-BPPFA	0	19	0

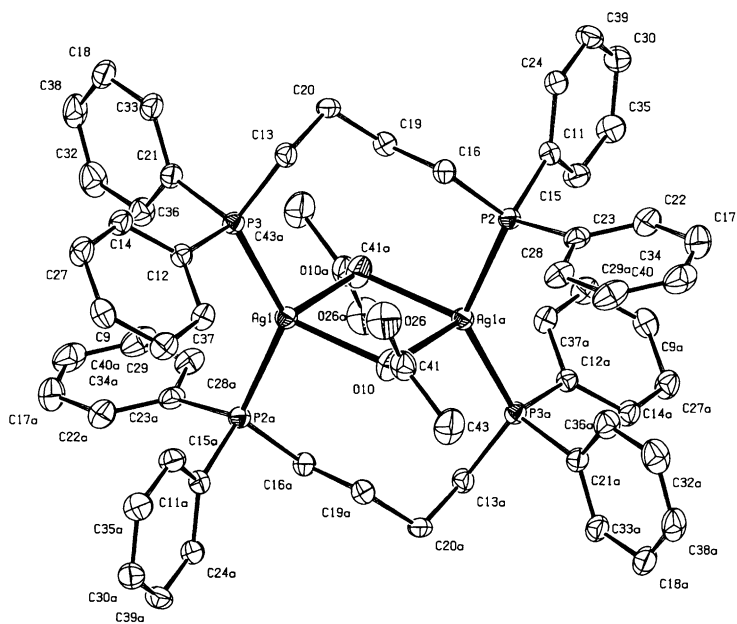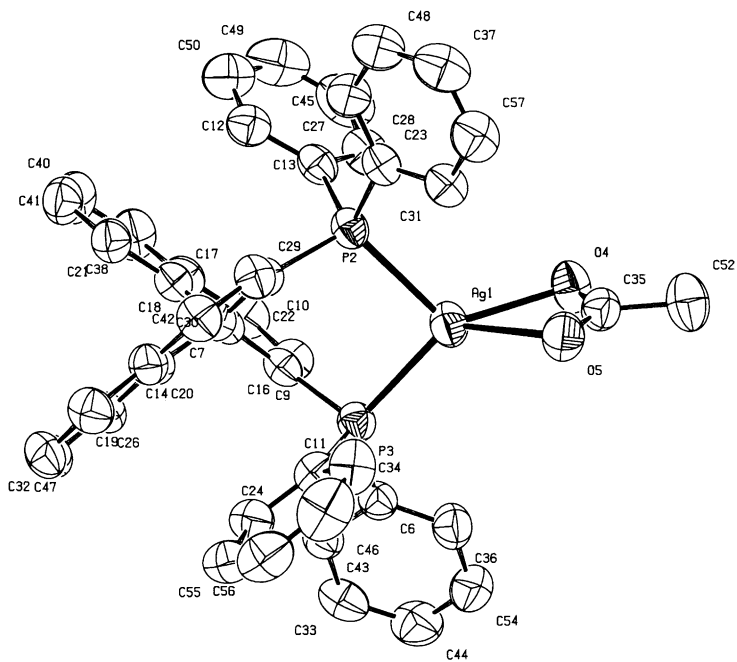[a] The reaction between benzaldehyde (50 eq.) and acetophenone silyl enol ether (100 eq.) performed in DMF at 25°C.

Fig. 3. The ORTEP drawing of [AgOAc(dppb)]₂.

Fig. 4. The ORTEP drawing of AgOAc((*S*)-BINAP).

Table 6

Crystallographic data for [Ag(OAc)(dppb)]$_2$ and AgOAc(BINAP)·CHCl$_3$

	[Ag(OAc)(dppb)]$_2$	AgOAc(BINAP)
Chemical formula	C$_{60}$ H$_{62}$ Ag$_2$ O$_4$ P$_4$	C$_{47}$ H$_{36}$ Ag Cl$_3$ O$_2$ P$_2$
Fw	1186.72	908.92
Diffractometer	Bruker SMART CCD	Bruker SMART CCD
Crystal system	Triclinic	Orthorhombic
Space group	$P\bar{1}$ (number 2)	$P2_12_12$ (number 18)
a (Å)	10.2536 (10)	16.1652 (9)
b (Å)	11.7167 (12)	24.0891 (13)
c (Å)	12.9938 (13)	10.8762 (6)
α (°)	65.590 (2)	
β (°)	71.166 (2)	
γ (°)	76.483 (2)	
V (Å^3)	1336.3 (2)	4235.2 (4)
Z	1	4
$\rho_{calculated}$ (g/cm^3)	1.475	1.425
μ (mm^{-1})	0.899	0.778
T (K)	100	298
λ (Mo $K\alpha$) (Å)	0.71073	0.71073
$2\theta_{max}$ (°)	56.36	58.28
Number of independent datas	5712	9335
Number of observed reflections (n_o) [$\|F_o\|^2 > 2.0\sigma(\|F\|^2)$]	5427	5918
Number of parameters refined (n_v)	317	537
R1 (observed reflections)[a] [$F^2 > 2\sigma(F^2)$]	0.0438	0.0477
wR2 (observed reflections)[b] (F^2)	0.1174	0.1082
GOF[c]	0.876	0.916

[a] $R1 = \sum(|F_o - (1/k)F_c|)/\sum |F_o|$.
[b] $wR2 = \left[\sum w(F_o^2 - (1/k)F_c^2)^2/\sum w|F_o^2|^2\right]$, $w = 1/[\sigma(F_o^2) + (0.0828P)^2 + 4.0051P]$ ([Ag(OAc)(dppb)]$_2$), $w = 1/[\sigma^2(F_o^2) + (0.00.0483P)^2 + 0.0000P]$ (AgOAc(BINAP)), $P = (F_o^2 + 2F_c^2)/3$.
[c] $GOF = \left[\sum w(F_o^2 - (1/k)F_c^2)^2/(n_o - n_v)\right]^{1/2}$.

The solid AgOAc-dppb complex was a binuclear complex bridged by acetate ion and phosphorous atoms of dppb ligand coordinated to silver atoms separately (Fig. 3). Concerning the crystal structure of AgOAc-diphosphine complexes only a few examples were known so far. The [AgOAc(dppm)]$_2$ [40] was reported to have the similar binuclear structure. As for AgNO$_3$ system, many diphosphine complexes were known with dppf [41], dppb [42], hexane (dpph) [43], and dppm [44] ligands. In these complexes diphosphine ligand coordinated to two silver atoms, thus, forming diphosphine bridged binuclear complex [45–50].[1] Therefore, we supposed that silver-diphosphine complexes generally form similar

diphosphine bridged complexes. To our knowledge, mononuclear complex (silver:diphosphine = 1:1 form) was scarce [51].[2] However, AgOAc-(S)-BINAP complex was a mononuclear complex (Fig. 4) different from those described above.

2.6. Structure of AgOAc-diphosphine complex in solution

In DMF or THF solution, AgPF$_6$-diphosphine complex formed an equilibrium state between several species described above.

Table 7 summarizes ^{31}P NMR data of AgOAc-diphosphine complexes and the number of the

---

[1] Several phosphine-bridged silver-diphosphine complexes were reported: AgCl complex; dppf [45]; dppp [46]; AgI complex [47]; AgClO$_4$-dppm complex [48]; AgOCOCH$_2$Ph-dppm complex [49]; AgNO$_3$-dppe complex [50].

[2] One example of mononuclear complex in AgCl system was reported. The ligand was 2,11-bis(diphenylphosphinomethyl)benzo-[c]phenanthrene.

Table 7
^{31}P NMR parameter for AgOAc-diphosphine complex in CDCl$_3$

Complex	Temperature (°C)	δ	$J_{^{107}Ag-^{31}P}$	$J_{^{109}Ag-^{31}P}$	P[a]	L[b]	
BINAP	25	11.63(dd)	342	397			
	−50	10.81(dd)	342	403	2	1	Major
		15.90(dd)	225	255	4	2	Minor
		4.75(dd)	676	796	1	0.5	Minor
Tol-BINAP	25	9.77(dd)	344	403			
	−50	10.81(dd)	349	407	2	1	Major
		15.88(dd)	226	262	4	2	Minor
		4.93(dd)	663	770	1	0.5	Minor
dppf	25	−5.16(d, br)		409			
	−50	−5.45(dd)	433	498	2	1	
dppp	25	0.17(s, br)					
	−50	−0.98(dd)	433	498	2	1	Major
		−6.26(dd)	218	253	4	2	Minor
dppb	25	1.01(s, br)					
	−50	0.34(dd)	420	491	2	1	
	−80	−0.58(dd)	433	492	2	1	In CH$_2$Cl$_2$

[a] The number of coordinated phosphorous atoms.
[b] The number of the coordinated ligands.

coordinated phosphorous atoms and ligand. AgOAc-(S)-BINAP and AgOAc-(S)-Tol-BINAP showed one sharp double doublet at 25°C, and lowering the temperature to −50°C three kinds of peaks were observed. Other complexes showed broad singlet or doublet peak at 25°C and one or two kinds of sharp double doublet at −50°C. These results show that these complexes are labile.

Equilibrium state of AgOAc-(S)-BINAP in CDCl$_3$ at −50°C is shown in Fig. 5a. The complex of 15.90 ppm peak has a coupling constant of 225 Hz (^{107}Ag–^{31}P) and is concluded to have four coordinated phosphorous atoms, that is, two BINAP ligands. Therefore, this complex is Ag((S)-BINAP)$_2$OAc. In AgPF$_6$-BINAP system, bis-BINAP species was a major component and was very stable and gave a sharp double doublet even at 25°C in ^{31}P NMR in solution. However, Ag((S)-BINAP)$_2$OAc species exists as a minor species and is in equilibrium with other Ag species and major species was 1:1 silver-BINAP complex.

This major complex has coordinative acetate anion (since this complex has a chemical shift different from [Ag((S)-BINAP)]PF$_6$), three possibilities are considered: the mononuclear (**2b-1**) similarly to

solid state structure, binuclear (**2b-2**) or polymeric complex (**2b-3**) (Fig. 6). We examined the possibility of scrambling of (S)-BINAP and (S)-Tol-BINAP in this 1:1 complex. AgOAc (1 eq.), (S)-BINAP (0.5 eq.) and (S)-Tol-BINAP (0.5 eq.) were mixed in CDCl$_3$ and this mixture was analyzed by ^{31}P NMR. The result was shown in Fig. 5b. In the chemical shift region of 1:1 complex, only two species were observed indicating the exact superposition of AgOAc-BINAP (**2b**) and AgOAc-Tol-BINAP (**2b′**) species. As 1:2 complex, AgOAc(BINAP)$_2$ (**2a**) and AgOAc(Tol-BINAP)$_2$ (**2a′**) were observed. All peaks could be assigned and no peaks were observed more intricate than double doublet except AgOAc((S)-BINAP)((S)-Tol-BINAP).[3] If **2b-2** and **2b-3** are present in solution, it is fully expected that more intricate peak appears in the region of 1:1 species, similarly to the

---

[3] We examined the synthesis of the Ag(I) complex from BINAP (1 eq.), Tol-BINAP (1 eq.), and AgOAc (1 eq.). ^{31}P NMR analysis of the mixture indicated the formation of three Ag(I) complexes. All species had coupling constants corresponding to four phosphorous atoms coordinated complex and were assigned as AgOAc(BINAP)$_2$, AgOAc(Tol-BINAP)$_2$ and AgOAc(BINAP)(Tol-BINAP).
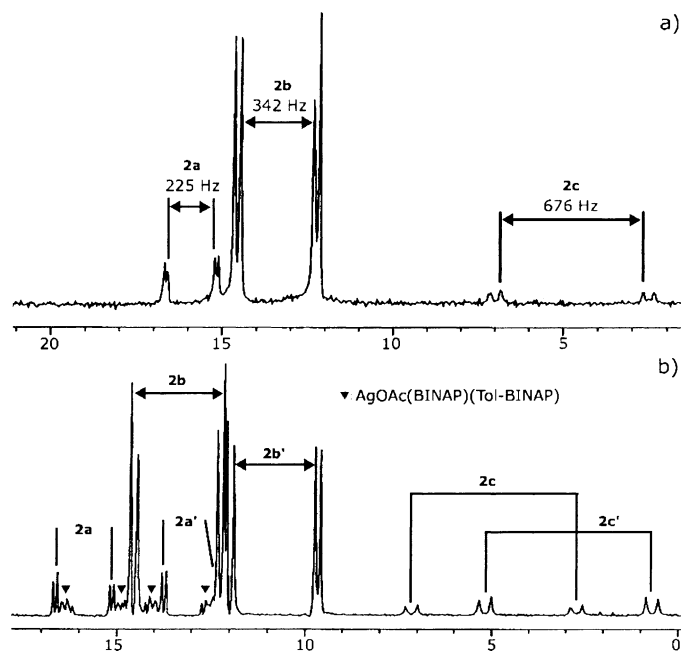
Fig. 5. ^{31}P NMR spectra of AgOAc-(S)-BINAP system: (a) ^{31}P NMR spectra of AgOAc-(S)-BINAP in CDCl$_3$ at −50°C; (b) spectra of the complexes prepared from AgOAc (1 eq.), (S)-BINAP (0.5 eq.), and (S)-Tol-BINAP (0.5 eq.) (**2a′**–**2c′** have (S)-Tol-BINAP ligand).

Ag((S)-BINAP)((S)-Tol-BINAP) species which was really observed. On addition of 1 eq. (S)-Tol-BINAP to the solution of AgOAc-(S)-BINAP 1:1 system, double doublet at 13.5 ppm largely diminished and **2a**, **2a′** and AgOAc((S)-BINAP)((S)-Tol-BINAP) were observed. Therefore, the 1:1 complex of 13.5 ppm (Fig. 5a) is concluded to be mononuclear (**2b-1**) one.

We also examined the scrambling experiment for AgOAc-dppb system. AgOAc-dppb and AgOAc-dppp complexes afforded double doublet signal with a large coupling constant ($J \sim 500$ Hz), respectively at −50°C in CDCl$_3$. AgOAc-dppb and AgOAc-dppp were mixed in CDCl$_3$ and the mixture was analyzed at −50°C. New eight doublets were observed in addition
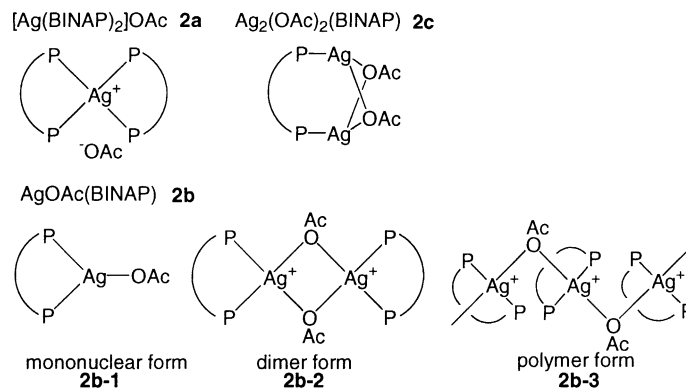

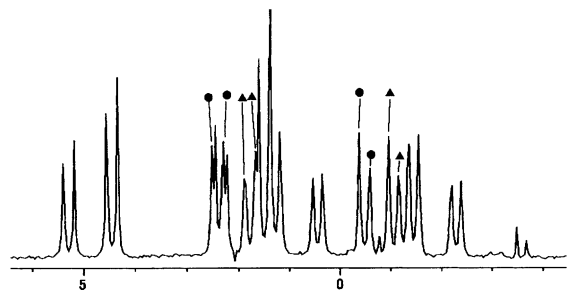Fig. 6. Structure of AgOAc-(S)-BINAP complex.

Fig. 7. Scrambling experiment between AgOAc-dppb and AgOAc-dppp: (●), AgOAc-dppp; (▲), AgOAc-dppb.

to AgOAc-dppb and AgOAc-dppp peaks. This result shows that AgOAc-dppb holds dimeric structure in solution similar to solid state structure (Fig. 7).

2.7. Reaction mechanism of Mukaiyama aldol reaction catalyzed by AgOAc-(S)-BINAP catalyst

By addition of DMF to the complex solution in CDCl$_3$ (0.4 eq. volume for CDCl$_3$), the peak of **2b-1** in ^{31}P NMR spectra became broad. This result shows that new equilibrium was caused by DMF. When benzaldehyde and nucleophile such as silyl enol ether or ketene silyl acetal were added, the peak form was changed to indicate that the substrate and nucleophile interact with the monomeric silver complex. Because of broadness of the peak, it was difficult to analyze the structure and equilibrium state.

Therefore, we examined ^{31}P NMR spectra of the complex in THF.[4] Although, **2a** indicated a broad peak at 25 and −50°C, sharp peaks were observed at −90°C. Addition of benzaldehyde to the solution at −90°C caused only a small change in the spectra (Fig. 8b). When ketene silyl acetal **3** was added to the above AgOAc-(S)-BINAP complex in THF, the spectra changed and new peaks appeared (Fig. 8c). The same spectra was observed by addition of the ketene silyl acetal to AgOAc-(S)-BINAP solution without benzaldehyde. The $J_{107_{Ag}-^{31}P}$ values of these species were 342 Hz (10.72 ppm), 338 Hz (10.23 ppm), 314 Hz (3.34 ppm) and 301 Hz (3.34 ppm), respectively. This

---

[4] We examined the Mukaiyama aldol reaction in THF. Although, the reaction activity was lower than in DMF, the aldol product was obtained in 78% yield and 11% e.e. (*R*) after 5 h at 25°C. The reaction in THF afforded the same optical yield and absolute configuration as those by the reaction in DMF.
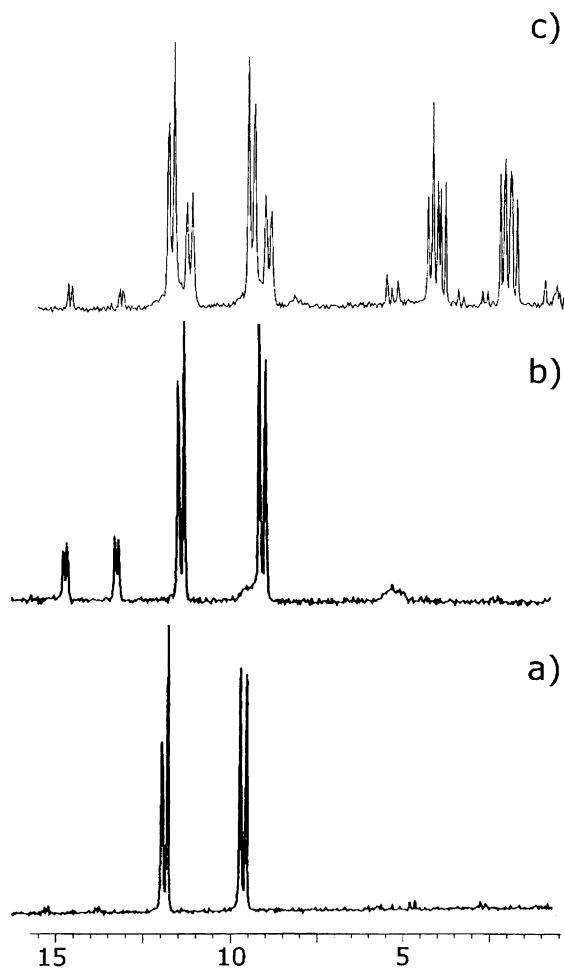

Fig. 8. ^{31}P NMR spectra of AgOAc-(S)-BINAP in THF at −90°C: (a) ^{31}P NMR spectra of AgOAc-(S)-BINAP in THF; (b) 50 eq. of benzaldehyde was added to (a); (c) 100 eq. of ketene silyl acetal **3** was added to (b).

shows that these Ag(I) species have one BINAP ligand. The spectra change caused only by the addition of ketene silyl acetal indicates that **2b-1** strongly interacts with ketene silyl acetal in THF. It suggests that the activation of ketene silyl acetal by **2b-1** occurs in solution of AgOAc-(S)-BINAP. These strong interaction of the nucleophile with AgOAc-(S)-BINAP species was not observed in the case of AgPF$_6$-(S)-BINAP system. With this AgOAc catalyst, silyl enol ether or ketene silyl acetal is very rapidly hydrolyzed in methanol to afford no aldol product at all, while with AgPF$_6$-(S)-BINAP catalyst the aldol product was

Table 8
The reactions in MeOH[a]

Entry	Ag complex	Yield (%)
1	AgOAc-(S)-BINAP	0[b]
2	AgPF$_6$-(S)-BINAP	4[b]
3	AgOTf-(S)-BINAP	32[b]

[a] The reaction between benzaldehyde (50 eq.) and acetophenone silyl enol ether (100 eq.) performed at 25°C
[b] Methanolysis of silyl enol ether also performed.

Fig. 9. UV–VIS spectra of AgOAc-(S)-BINAP in DMF.

obtained in 4% yield and with AgOTf-(S)-BINAP catalyst the aldol reaction occurred in 32% yield in methanol (Table 8). This will indicate the different degree of the activation of the nucleophile by Ag(I) species. The presence of four peaks will suggest that coordination mode of the ketene silyl acetal is not simple and coordination of the nucleophile by silyl oxygen or carbon–carbon double bond is possible.

We observed the formation of silver enolate species in a wet THF-d_8 solution using cationic AgPF$_6$-BINAP catalyst by ^{1}H NMR [37]. By the coordination to the AgOAc-(S)-BINAP species, the nucleophile is expected to be activated to afford the silver enolate species as an intermediate in solution. However, ^{1}H NMR analysis in DMF-d_7, THF-d_8 and CDCl$_3$ at low temperature, did not indicate the formation of the silver enolate species in solution.

This interaction of the nucleophile with AgOAc-BINAP species was also observed in UV–VIS spectra (Fig. 9). In the DMF solution of AgOAc-(S)-BINAP system in the presence of the 50 equivalent substrate, no absorption maxima was observed in 350–600 nm region. However, addition of ketene silyl acetal **3** to the above solution afforded the new absorption maxima at 413 nm with an isobestic point at 366 nm. This absorption was also observed without the substrate **4**. The peak at 413 nm may be ascribed to MLCT band of the AgOAc-BINAP - **3** complex.

While AgPF$_6$-(S)-BINAP system afforded fairly high enantioselectivity in the reaction of benzaldehyde and acetophenone silyl enol ether, the catalyst AgOAc-(S)-BINAP afforded low enantioselectivity with an inversion of chiral induction. The reaction by AgCl-(S)-BINAP catalyst also indicated the same chiral induction as that by AgOAc-(S)-BINAP though the reactivity of AgCl catalyst is much lower than that of AgOAc species. NMR and UV–VIS spectra
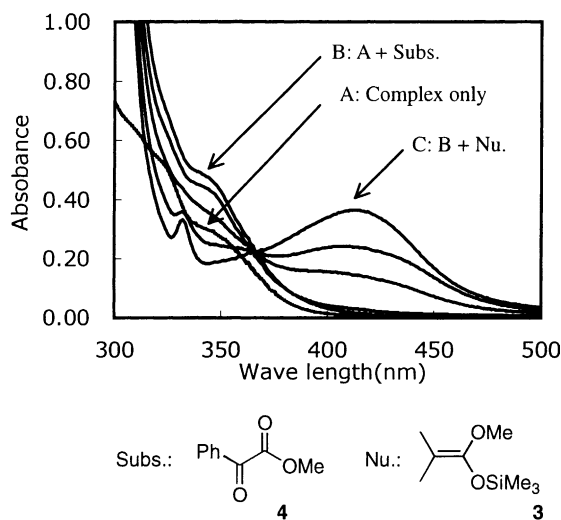
indicated that this AgOAc-BINAP species interact strongly with nucleophiles (silyl enol ether or ketene silyl acetal) to activate the nucleophile. In the reaction of benzaldehyde using silyl enol ethers **5** and **6** by AgOAc-(S)-BINAP catalyst, the reaction proceeded in a *syn*-selective manner for both nucleophiles (Table 4). These results strongly suggest the reaction proceeded through an acyclic transition state [52–54]. We consider that nucleophile was activated by silver atom and acetate anion [55–57],[5] and the reaction proceeded by the direct attack of Ag-nucleophile complex to the substrate via acyclic transition state (Fig. 10).

3. Experimental

3.1. General Method

^{1}H NMR and ^{31}P NMR spectra were obtained with a JEOL-EX270 and JEOL-LA400 NMR spectrometer using tetramethylsilane (Me$_4$Si) as an internal standard and 85% H$_3$PO$_4$ as an external standard, respectively. *J*-values are given in Hz. Mass spectra were recorded on a JEOL LX-1000 in *m*-nitrobenzyl al-

---

[5] Several examples were known of the activation of silicon atom by carboxylates or alkoxides; Sn promoted Aldol reaction [55]; Pd-catalyzed π-allyl alkylation with BSA [56]; trifluoromethylation with TMS-CF$_3$ [57].
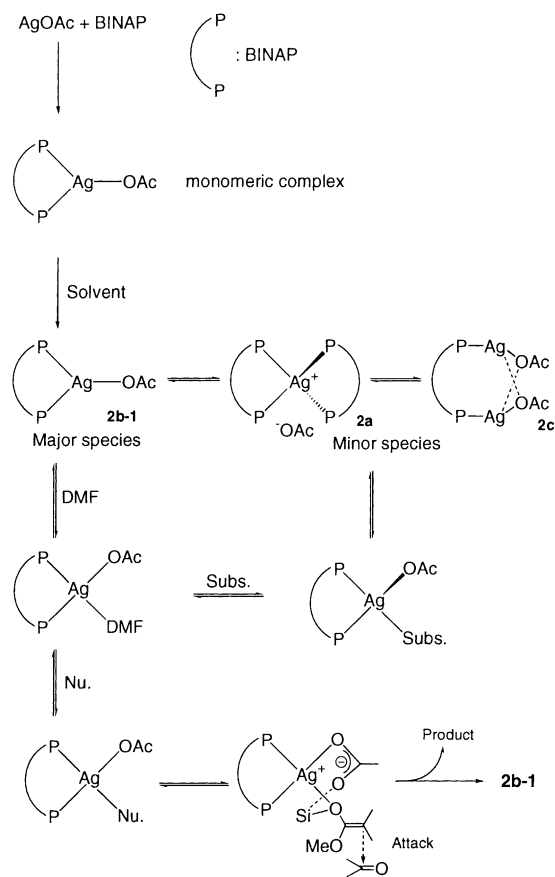
Fig. 10. Equilibrium state and proposed reaction mechanism of AgOAc-(S)-BINAP system.

cohol matrix with a fast atom bombardment ionization method. Column chromatography was performed with Merck silica gel (230–400 mesh). HPLC for the separation of enantiomers was carried out on a Shimadzu LC-6A and LC-10A chromatograph using Chiralcel OB-H and OD-H columns (Daicel Chemical Industry) at room temperature. The mobile phase was n-hexane/propan-2-ol (9:1) and detection was done by a UV–VIS detector and polarimeter detector.

3.2. Experimental procedure of Mukaiyama aldol reaction

A typical experimental procedure for silver(I)-catalyzed asymmetric Mukaiyama aldol reaction of benzaldehyde and acetophenone silyl enol ether is as

follows. To a mixture of $AgPF_6$ (4.0 mg, 0.013 mmol) and (S)-BINAP (8.4 mg 0.013 mmol) was added DMF (206 μl, solvent) under nitrogen atmosphere and the solution was stirred at room temperature for 10 min. Benzaldehyde (69 μl, 0.67 mmol, substrate) was added to the solution and the mixture was stirred for 10 min. Acetophenone silyl enol ether (276 μl, 1.35 mmol, nucleophile) was added and the mixture was stirred at 25°C for 2 h. It was filtrated through a short silica gel column (EtOAc/hexane (1:1)) and concentrated under reduced pressure to afford clear oil. The oil was hydrolyzed with 1 M HCl THF/water (1:1) solution, extracted with diethylether, dried over anhydrous sodium sulfate, concentrated in vacuo to give pale clear oil. This oil was purified by silica gel column chromatography (EtOAc/hexane (1:1)).

3.3. Aldol reaction product

The yield was determined by ^1H NMR analysis [58,59].[6] Enantiomeric excess was determined by HPLC analysis using Daicel Chiralcel OB-H, or OD-H. The absolute configuration of the products was determined by their optical rotation.

3.4. 1-Hydroxy-1,3-diphenyl-3-propanone

^1H NMR ($CDCl_3$, 270 MHz) δ 3.38 (d, 2H, $J =$ 5.9 Hz, CH_2), 3.56 (d, 1H, $J =$ 3.0 Hz, OH), 5.35 (dt, 1H, $J =$ 3.0 Hz, 5.9 Hz, CH), 7.26–7.62 (m, 8H, Ph), 7.95 (d, 2H, $J =$ 7.3 Hz, Ph). FAB–MS calcd. for $C_{15}H_{14}O_2$, 226 (M^+); found 227 (($M +$ 1)$^+$), 209 ((M-OH)$^+$), HPLC (OB-H column, eluent; hexane/2-propanol (9:1), flow rate 0.9 ml/min) $t_R =$ 22.5 min ((R)-isomer), $t_R =$ 33.5 min ((S)-isomer); (OD-H column, eluent; hexane/2-propanol (9:1), flow rate 0.5 ml/min) $t_R =$ 22.5 min ((R)-isomer), $t_R =$ 24.5 min ((S)-isomer).

3.5. 1-Hydroxy-1-(1-naphthyl)-3-phenyl-3-propanone

^1H NMR (270 MHz, $CDCl_3$) δ 3.42–3.61 (m, 2H, CH_2), 3.70 (d, 1H, $J =$ 3.0 Hz, OH), 6.15 (m, 1H, CH), 7.25–8.07 (m, 12H, Ar), HPLC (OB-H column, eluent; hexane/2-propanol (9:1), flow rate

---

[6] As for aldol reaction product see also [37].

0.9 ml/min), t_R = 32.8 min ((+)-isomer), t_R = 60.3 min ((−)-isomer).

3.6. 1-Hydroxy-1-(2-naphthyl)-3-phenyl-3-propanone

^{1}H NMR (270 MHz, CDCl$_3$) δ 3.46 (m, 2H, CH$_2$), 3.70 (s, 1H, OH), 5.52 (m, 1H, CH), 7.25–7.98 (m, 12H, Ph), HPLC (OB-H column, eluent; hexane/2-propanol (9:1), flow rate 0.9 ml/min), t_R = 42.2 min ((+)-isomer), t_R = 52.5 min ((−)-isomer).

3.7. 1-Hydroxy-2-methyl-1,3-diphenyl-3-propanone

^{1}H NMR (CDCl$_3$, 270 MHz) *anti*-isomer: δ 1.07 (d, 3H, J = 7.2 Hz, CH$_3$), 3.6–3.8 (m, 1H, C*H*CH$_3$), 4.99 (d, 1H, J = 8.3 Hz, C*H*OH), 7.2–8.2 (m, 10H, Ph), *syn*-isomer: δ 1.19 (d, 3H, J = 7.2 Hz, CH$_3$), 3.6–3.8 (m, 1H, C*H*CH$_3$), 5.23 (d, 1H, J = 3.3 Hz, C*H*OH), 7.2–8.2 (m, 10H, Ph), HPLC (OD-H column, eluent; hexane/2-propanol (9:1), flow rate 0.5 ml/min), t_R = 13.3 min (*syn* (−)-isomer), t_R = 14.8 min (*syn* (+)-isomer), t_R = 15.9 min (*anti* (−)-isomer), t_R = 17.5 min (*anti* (+)-isomer).

3.8. 2-(α-Hydroxybenzyl)cyclohexanone

^{1}H NMR (CDCl$_3$, 270 MHz) *anti*-isomer: δ 1.29–2.62 (m, 9H, c-C$_6$H$_9$), 3.96 (s, 1H, OH), 4.78 (d, 1H, J = 8.8 Hz, CH), 7.23–7.36 (m, 5H, Ph), *syn*-isomer: δ 1.29–2.62 (m, 9H, c-C$_6$H$_9$), 3.01 (s, 1H, OH), 5.39 (s, 1H, CH), 7.23–7.36 (m, 5H, Ph), HPLC (OD-H column, eluent; hexane/2-propanol (9:1), flow rate 0.5 ml/min), t_R = 13.3 min (*syn* (−)-isomer), t_R = 14.8 min (*syn* (+)-isomer), t_R = 15.9 min (*anti*-isomer), t_R = 17.5 min (*anti*-isomer).

3.9. Preparation of [Ag(BINAP)$_2$]PF$_6$ (**1a**)

To a Schlenck tube (S)-BINAP (258 mg, 0.414 mmol) and AgPF$_6$ (49.6 mg, 0.196 mmol) were placed under a nitrogen atmosphere. The schlenck tube was charged with THF (2 ml) and the mixture was stirred for 30 min to give a white suspension. The solvent was removed in reduced pressure and white solid was obtained. This solid was dissolved in CHCl$_3$ (5 ml) and filtered. The filtrate was concentrated for 1 ml, Et$_2$O (10 ml) was added, and cooled at −30°C. The clear crystals

formed and were filtered, [Ag((S)-BINAP)$_2$]PF$_6$ (**1a**) was gave as a clear crystal in 97% yield.

^{31}P NMR at 25°C (162 MHz, CDCl$_3$) δ 17.4 (dd, $J_{^{109}Ag–^{31}P}$ = 260 Hz, $J_{^{107}Ag–^{31}P}$ = 226Hz), −143 (m, $J_{^{19}F–^{31}P}$ = 166 Hz, PF$_6$), FAB–MS calculated for C$_{88}$H$_{64}$AgF$_6$P$_5$, 1353 ((M-PF$_6$)$^+$); found, 1353 ((M-PF$_6$)$^+$), 731 ((M-BINAP-PF$_6$)$^+$), elemental analysis; calculated C, 70.55; H, 4.31, found, C, 70.27; H, 4.54.

3.10. Preparation of AgOAc-(S)-BINAP complex

To a Schlenck tube (S)-BINAP (200 mg, 0.32 mmol) and AgOAc (53.6 mg, 0.32 mmol) were placed under a nitrogen atmosphere. The Schlenck tube was charged with THF (5 ml) and the mixture was stirred for 30 min to give a white suspension. The solvent was removed under reduced pressure and white solid was obtained. This solid was dissolved in CH$_2$Cl$_2$ (5 ml) and filtered. The filtrate was concentrated to 1 ml and Et$_2$O (10 ml) was added, and cooled at −30°C. Formed crystals were filtered to give AgOAc-(S)-BINAP as clear crystal in 93% yield. The single crystal was obtained by slow recrystallization from CHCl$_3$–cyclohexane (1:6) at room temperature.

^{31}P NMR at 25°C (162 MHz, CDCl$_3$) δ 11.63 (dd, $J_{^{109}Ag–^{31}P}$ = 397 Hz, $J_{^{107}Ag–^{31}P}$ = 342 Hz), at −50°C (162 MHz, CDCl$_3$) δ 15.90 (dd, $J_{^{109}Ag–^{31}P}$ = 255 Hz, $J_{^{107}Ag–^{31}P}$ = 225 Hz, minor species Ag(BINAP)$_2$OAc), 10.81 (dd, $J_{^{109}Ag–^{31}P}$ = 403 Hz, $J_{^{107}Ag–^{31}P}$ = 342 Hz, major species, Ag(BINAP)OAc), 4.75 (dd, $J_{^{109}Ag–^{31}P}$ = 796 Hz, $J_{^{107}Ag–^{31}P}$ = 676 Hz, minor species, Ag$_2$(BINAP)(OAc)$_2$), FAB–MS calculated for C$_{46}$H$_{35}$AgO$_2$P$_2$ (AgOAc(BINAP)), 791 ((M)$^+$); found, 731 ((M-OAc)$^+$), elemental analysis; calculated for AgOAc(BINAP) C, 69.97; H, 4.47, found, C, 69.89; H, 4.57.

3.11. Preparation of [AgOAc(dppb)]$_2$ complex

[AgOAc(dppb)]$_2$ was obtained as a clear crystal by same procedure for AgOAc-(S)-BINAP complex. The single crystal was obtained by recrystallization from CH$_2$Cl$_2$–Et$_2$O (1:10) solution at −30°C.

^{31}P NMR at 25°C (162 MHz, CDCl$_3$) δ 1.01 (s, br), at −50°C (162 MHz, CDCl$_3$) δ 0.34 (dd, $J_{^{109}Ag–^{31}P}$ = 491 Hz, $J_{^{107}Ag–^{31}P}$ = 420 Hz), at −80°C (162 MHz, CH$_2$Cl$_2$) δ −0.58 (dd, $J_{^{109}Ag–^{31}P}$ =

492 Hz, $J_{107_{Ag}-31_P} = 433$ Hz) FAB–MS calculated for $C_{62}H_{66}Ag_2O_4P_4$ ([AgOAc(dppb)]$_2$), 1214 ((M)$^+$); found, 1154 ((M-OAc)$^+$), 985 ((M-AgOAc)$^+$), 545 ((M-AgOAc-dppb)$^+$), elemental analysis; calculated for [AgOAc(dppb)]$_2$·H$_2$O C, 60.27; H, 5.31, found, C, 60.20; H, 5.39. TG–DTA analysis indicated the presence of one H$_2$O.

3.12. Preparation of AgOAc-dppf complex

AgOAc-dppf was obtained as an orange crystal by the same procedure for AgOAc-(*S*)-BINAP complex.

^{31}P NMR at 25°C (162 MHz, CDCl$_3$) δ −5.16 (d, br, $J_{Ag-P} = 409$ Hz), at −50°C (162 MHz, CDCl$_3$) δ −5.45 (dd, $J_{109_{Ag}-31_P} = 498$ Hz, $J_{107_{Ag}-31_P} = 433$ Hz), FAB–MS calculated for $C_{72}H_{66}Ag_2Fe_2O_4P_4$ ([AgOAc(dppf)]$_2$), 1446 ((M)$^+$); found, 1386 ((M-OAc)$^+$), 1217 ((M-Oac-AgOAc)$^+$), 661 ((M-OAc-AgOAc-dppf)$^+$), elemental analysis; calculated for [AgOAc(dppf)]$_2$·H$_2$O C, 59.21; H, 4.42, found, C, 58.90; H, 4.34.

3.13. Preparation of AgOAc-dppp complex

AgOAc-dppp was obtained as clear powder by the same procedure for AgOAc-(*S*)-BINAP complex.

^{31}P NMR at 25°C (162 MHz, CDCl$_3$) δ 0.17 (s, br), at −50°C (162 MHz, CDCl$_3$) δ −0.98 (dd, $J_{109_{Ag}-31_P} = 498$ Hz, $J_{107_{Ag}-31_P} = 433$ Hz, major species, AgOAc(dppp)), −6.26 (dd, $J_{109_{Ag}-31_P} = 253$ Hz, $J_{107_{Ag}-31_P} = 218$ Hz, minor species, AgOAc(dppp)$_2$) FAB–MS calculated for $C_{60}H_{62}Ag_2O_4P_4$ ([AgOAc(dppp)]$_2$), 1186 ((M)$^+$); found, 1126 ((M-OAc)$^+$), 957 ((M-OAc-AgOAc)$^+$), 531 ((M-OAc-AgOAc-dppf)$^+$), elemental analysis; calculated for [AgOAc(dppp)]$_2$·H$_2$O C, 59.20; H, 5.14, found, C, 59.00; H, 5.14.

3.14. X-ray crystallography

A colorless single crystal was mounted on Bruker SMART CCD diffractometer. Data collection was performed by using an ω scan in steps of 0.3°. Determination of the space group was performed by the systematic absences, while the cell constants were refined after data collection with SAINT program [60]. The collected intensities were corrected for Lorentz and polarization factors by SAINT program [60]. An empirical absorption correction was also applied using the SADABS program [61].

The structure was solved by direct and Fourier methods. The data were refined by full-matrix least squares [62], minimizing the function $\sum w \left[F_o^2 - (1/k) F_c^2 \right]^2$. The handedness of structure was tested by refining the Flack parameter [63,64].

The calculations of initial structure were carried out by using PC version of SIR92 [65] [7] and the refinement was carried out by using SHELX-97 programs [62]. The crystallographic data were listed in Table 6.

4. Conclusion

We examined structure and equilibrium state in solution to understand the reaction mechanism. We found a difference in equilibrium state in solution between AgPF$_6$ system and AgOAc system. In AgPF$_6$ system, [Ag(BINAP)$_2$]PF$_6$ (**1a**) was a major species, but **1a** was stable and inactive. [Ag(BINAP)]PF$_6$ (**1b**) which exists as a minor species was active species. From the change in NMR spectra by addition of substrate and nucleophile and high enantioselectivity in the case of AgPF$_6$-BINAP, the reaction is considered to proceed through the six-membered transition state. In AgOAc-diphosphine systems, mode of coordination of diphosphine differs depending on the structure of diphosphines. AgOAc-dppb formed a diphosphine bridged dimer in the solid state and in solution. AgOAc-(*S*)-BINAP complex formed phosphine chelated monomeric complex in solid state and in solution, 1:1 monomeric AgOAc((*S*)-BINAP) complex exists as a major species and interacts strongly with the nucleophile to cause the activation and the reaction was considered to proceed through the acyclic transition state by the direct attack of the Ag-nucleophile species to the substrate.

References

[1] T. Bach, Angew. Chem., Int. Ed. Engl. 33 (1994) 417.
[2] S.G. Nelson, Tetrahedron Asymmetry 9 (1998) 357.
[3] T.D. Machajewski, C.-H. Wong, Angew. Chem., Int. Ed. Engl. 39 (2000) 1353.

---

[7] SIR92: a program for crystal structure solution.

[4] R. Hara, T. Mukaiyama, Chem. Lett. (1989) 1909.

[5] T. Mukaiyama, A. Inubushi, S. Suda, R. Hara, S. Kobayashi, Chem. Lett. (1990) 1015.

[6] T. Mukaiyama, Angew. Chem., Int. Ed. Engl. 16 (1977) 817.

[7] E.M. Carreira, R.A. Singer, W. Lee, J. Am. Chem. Soc. 116 (1994) 8837.

[8] K. Mikami, S, Matsukawa, J. Am. Chem. Soc. 116 (1994) 4077.

[9] K. Mikami, S, Matsukawa, J. Am. Chem. Soc. 115 (1993) 7039.

[10] S. Kobayashi, A. Ohtsubo, T. Mukaiyama, Chem. Lett. (1991) 831.

[11] S. Kobayashi, Y. Fujishita, T. Mukaiyama, Chem. Lett. (1990) 1455.

[12] S. Kobayashi, Y. Fujishita, T. Mukaiyama, Chem. Lett. (1989) 2069.

[13] T. Mukaiyama, T. Sano, S. Kobayashi, Chem. Lett. (1989) 1757.

[14] S. Kobayashi, T. Sano, T. Mukaiyama, Chem. Lett. (1989) 1319.

[15] K. Ishihara, T. Maruyama, M. Mouri, Q. Gao, K. Furuta, H. Yamamoto, Bull. Chem. Soc. Jpn. 66 (1993) 3483.

[16] K. Furuta, T. Maruyama, H. Yamamoto, J. Am. Chem. Soc. 113 (1991) 1041.

[17] E.J. Corey, C.L. Cywin, T.D. Roper, Tetrahedron Lett. 33 (1992) 6907.

[18] S. Kiyooka, Y. Kaneko, K. Kume, Tetrahedron Lett. 33 (1992) 4927.

[19] E.R. Parmee, Y. Hong, O. Tempkin, S. Masamune, Tetrahedron Lett. 33 (1992) 1729.

[20] M. Sodeoka, K. Ohrai, M. Shibasaki, J. Org. Chem. 60 (1995) 2648.

[21] M. Sodeoka, R. Tokunoh, F. Miyazaki, E. Hagiwara, M. Shibasaki, Synlett (1997) 463.

[22] K. Manabe, Y. Mori, T. Wakabayashi, S. Nagayama, S. Kobayashi, J. Am. Chem. Soc. 122 (2000) 7202.

[23] S. Kobayashi, S. Nagayama, J. Am. Chem. Soc. 120 (1998) 2985.

[24] S. Kobayashi, H. Ishitani, M. Ueno, J. Am. Chem. Soc. 120 (1998) 431.

[25] S. Kobayashi, S. Nagayama, J. Org. Chem. 62 (1997) 232.

[26] S. Kobayashi, H. Iwao, H. Ishitani, M. Araki, Synlett (1993) 472.

[27] S. Kobayashi, T. Busujima, J. Am. Chem. Soc. 120 (1998) 8287.

[28] T. Hayashi, M. Sawamura, Y. Ito, Tetrahedron 48 (1992) 1999.

[29] A. Togni, S.D. Pastor, J. Org. Chem. 55 (1990) 1649.

[30] M. Sawamura, H. Hamashima, Y. Ito, J. Org. Chem. 55 (1990) 5935.

[31] A. Yanagisawa, A. Ishiba, H. Nakashima, H. Yamamoto, Synlett (1997) 88.

[32] A. Yanagisawa, Y. Matsumoto, H. Nakashima, K. Asakawa, H. Yamamoto, J. Am. Chem. Soc. 119 (1997) 9319.

[33] Y. Ito, M. Sawamura, E. Shirakawa, K. Hayashizaki, T. Hayashi, Tetrahedron 44 (1988) 5253.

[34] A. Yanagisawa, H. Nakashima, A. Ishiba, H. Yamamoto, J. Am. Chem. Soc. 118 (1996) 4723.

[35] A. Yanagisawa, Y. Matsumoto, K. Asakawa, H. Yamamoto, J. Am. Chem. Soc. 121 (1999) 892.

[36] A. Yanagisawa, Y. Nakatsuka, K. Asakawa, H. Kageyama, H. Yamamoto, Synlett (2001) 69.

[37] M. Ohkouchi, M. Yamaguchi, T. Yamagishi, Enantiomer 5 (2000) 71.

[38] E.L. Muetterties, C.W. Alegranti, J. Am. Chem. Soc. 84 (1972) 6386.

[39] R.G. Goel, P. Pilon, Inorg. Chem. 17 (1978) 2876.

[40] S.P. Neo, Z.-Y. Zhou, T.C.W. Mak, T.S.A. Hor, Inorg. Chem. 34 (1995) 520.

[41] T.S.A. Hor, S.P. Neo, C.S. Tan, T.C.W. Mak, K.W.P. Leung, R.-J. Wang, Inorg. Chem. 31 (1992) 4510.

[42] Y. Runina, H. Yimin, X. Baoyu, W. Dobgmei, J. Douman, Trans. Met. Chem. 21 (1996) 28.

[43] S. Kitagawa, M. Kondo, S. Kawata, S. Wada, M. Maekawa, M. Munakata, Inorg. Chem. 34 (1995) 1455.

[44] E.R.T. Tiekink, Acta Crystallogr., Sect. C 46 (1990) 1933.

[45] K. Yang, S.G. Bott, M.G. Richmond, J. Chem. Cryst. 25 (1995) 263.

[46] A. Cassel, Acta Crystallogr., Sect. B 32 (1976) 2521.

[47] A. Cassel, Acta Crystallogr., Sect. B 31 (1975) 1194.

[48] B.H. Ahrens, P.G. Jones, Acta Crystallogr., Sect. C 54 (1998) 16.

[49] T.S.A. Hor, S.P. Neo, C.S. Tau, T.C.W. Mak, K.W.P. Leung, R.-J. Wang, Inorg. Chem. 31 (1992) 4510.

[50] E.R.J. Tiekink, Acta Crystallogr., Sect. C 46 (1990) 1933.

[51] M. Barrow, H.B. Burgi, M. Camalli, F. Caruso, E. Fischer, L.M. Venanzi, L. Zambonell, Inorg. Chem. 22 (1983) 2356.

[52] Y. Li, M.N. Paddon-Row, K.N. Houk, J. Org. Chem. 55 (1990) 481.

[53] A. Bernardi, A.M. Capelli, C. Gennari, J.M. Goodman, I. Paterson, J. Org. Chem. 55 (1990) 3576.

[54] S.E. Denmark, B.R. Henke, J. Am. Chem. Soc. 113 (1991) 2177.

[55] T. Mukaiyama, H. Uchiro, S. Kobayashi, Chem. Lett. (1989) 1757

[56] B.M. Trost, D.J. Murphy, Organometallics 4 (1985) 1143.

[57] R. Krishnamurti, D.R. Bellew, G.K.S. Parakash, J. Org. Chem. 56 (1991) 984.

[58] K. Ishihara, T. Maruyama, M. Mouri, Q. Gao, K. Furuta, H. Yamamoto, Bull. Chem. Soc. Jpn. 66 (1993) 3483.

[59] K. Ishihara, N. Hanaki, M. Funahashi, M. Miyata, H. Yamamoto, Bull. Chem. Soc. Jpn. 68 (1995) 1721.

[60] SAINT: SAX Area-Detector Integration, Siemens Analytical Instrumentation, Madison, WI, 1996.

[61] G.M. Sheldrick, SADABS: Area-Detector Absorption Correction, Universität Göttingen, Göttingen, Germany, 1996.

[62] G.M. Sheldrick, SHELX-97: Structure Solution and Refinement Package, Universität Göttingen, Göttingen, Germany, 1997.

[63] H.D. Flack, Flack X-parameter, Acta Crystallogr., Sect. A 39 (1983) 876.

[64] G. Bernardinelli, H.D. Flack, Acta Crystallogr., Sect. A 41 (1985) 500.

[65] A. Altomare, G. Cascarano, C. Giacovazzo, A. Guagliardi, J. Appl. Crystallogr. 26 (1993) 343.